



HAL
open science

Targeting DMPK with antisense oligonucleotide improves muscle strength in myotonic dystrophy type 1 mice

Dominic Jauvin, Jessina Chrétien, Sanjay Pandey, Laurie Martineau, Lucille Revillod, Guillaume Bassez, Aline Lachon, A. Robert Macleod, Geneviève Gourdon, Thurman Wheeler, et al.

► **To cite this version:**

Dominic Jauvin, Jessina Chrétien, Sanjay Pandey, Laurie Martineau, Lucille Revillod, et al.. Targeting DMPK with antisense oligonucleotide improves muscle strength in myotonic dystrophy type 1 mice. *Molecular Therapy - Nucleic Acids*, 2017, 7, pp.465-474. 10.1016/j.omtn.2017.05.007 . hal-03832497

HAL Id: hal-03832497

<https://hal.science/hal-03832497v1>

Submitted on 27 Oct 2022

HAL is a multi-disciplinary open access archive for the deposit and dissemination of scientific research documents, whether they are published or not. The documents may come from teaching and research institutions in France or abroad, or from public or private research centers.

L'archive ouverte pluridisciplinaire **HAL**, est destinée au dépôt et à la diffusion de documents scientifiques de niveau recherche, publiés ou non, émanant des établissements d'enseignement et de recherche français ou étrangers, des laboratoires publics ou privés.



Distributed under a Creative Commons Attribution - NonCommercial - NoDerivatives 4.0 International License

Targeting *DMPK* with Antisense Oligonucleotide Improves Muscle Strength in Myotonic Dystrophy Type 1 Mice

Dominic Jauvin,¹ Jessina Chrétien,¹ Sanjay K. Pandey,^{2,3} Laurie Martineau,¹ Lucille Revillod,⁴ Guillaume Bassez,⁴ Aline Lachon,⁵ A. Robert MacLeod,² Geneviève Gourdon,⁵ Thurman M. Wheeler,⁶ Charles A. Thornton,⁷ C. Frank Bennett,² and Jack Puymirat^{1,8}

¹Laval University Experimental Organogenesis Center/LOEX, Enfant-Jésus Hospital, Québec, QC G1J 1Z4, Canada; ²Ionis Pharmaceuticals, Inc., Carlsbad, CA 92010, USA; ³Triangulum Biopharma, San Diego, CA 92121, USA; ⁴INSERM U955, Neuromuscular Reference Center, Henri-Mondor Hospital, Créteil 94000, France; ⁵INSERM U781, Imagine Institute, Paris 75015, France; ⁶Massachusetts General Hospital, Boston, MA 02114-3117, USA; ⁷University of Rochester Medical Center, Rochester, NY 14642, USA; ⁸Department of Neurological Sciences CHU de Québec-Laval University, Enfant-Jésus Hospital, Québec, QC G1J 1Z4, Canada

Myotonic dystrophy type 1 (DM1), a dominant hereditary muscular dystrophy, is caused by an abnormal expansion of a (CTG)_n trinucleotide repeat in the 3' UTR of the human dystrophia myotonica protein kinase (*DMPK*) gene. As a consequence, mutant transcripts containing expanded CUG repeats are retained in nuclear foci and alter the function of splicing regulatory factors members of the MBNL and CELF families, resulting in alternative splicing misregulation of specific transcripts in affected DM1 tissues. In the present study, we treated DMSXL mice systemically with a 2'-4'-constrained, ethyl-modified (ISIS 486178) antisense oligonucleotide (ASO) targeted to the 3' UTR of the *DMPK* gene, which led to a 70% reduction in CUG^{exp} RNA abundance and foci in different skeletal muscles and a 30% reduction in the heart. Furthermore, treatment with ISIS 486178 ASO improved body weight, muscle strength, and muscle histology, whereas no overt toxicity was detected. This is evidence that the reduction of CUG^{exp} RNA improves muscle strength in DM1, suggesting that muscle weakness in DM1 patients may be improved following elimination of toxic RNAs.

INTRODUCTION

Myotonic dystrophy type 1 (DM1), the most common form of muscular dystrophy in adults, with an incidence of 1:15,000, is a multisystemic disorder characterized by myotonia, progressive muscle wasting, cardiac conduction defects, as well as endocrine deficiencies and cognitive impairments.¹ A severe congenital form (CDM1) of this disease is characterized by neonatal hypotonia, facial weakness, respiratory and feeding difficulties, and high neonatal mortality (16% versus 19:1,000 in the population). Available data suggest that CDM1 seems to be caused by delayed skeletal muscle and brain maturation,¹⁻⁴ whereas the adult form of DM1 appears to result from a degenerative process.

DM1 is caused by an expanded (CTG)_n repeat, where *n* varies from 50 to several thousand, in the 3' UTR of the dystrophia myotonica protein kinase (*DMPK*) gene.⁵ The most commonly accepted mecha-

nistic explanation is that the nuclear accumulation of transcripts containing CUG expansions sequesters the RNA-binding protein *MBNL1* and stabilizes *CELF1* via hyperphosphorylation.⁶⁻¹¹ The de-regulated expression and activity of these RNA-binding proteins in individuals affected by DM1 leads to perturbations in the alternative splicing of key genes.^{7,12} The extent of the contribution of spliceopathy to CDM1 pathogenesis, however, remains unclear.

Transgenic mouse models have been developed to investigate DM1 etiology.¹³⁻¹⁵ Among these models, the HSA^{LR} mouse expressing 250 CTG repeats under the human skeletal actin promoter¹³ and the DMSXL mouse, which harbors a mutant form of the human *DMPK* gene that carries >1,000 CTG repeats and is under the regulation of its own promoter. Homozygous DMSXL mice display several phenotypical manifestations of the disease and provide the only available DM1 model for screening of ASOs targeting *DMPK* regions outside the repeats.^{15,16}

It was previously shown that a steric blocking ASO targeting the CUG^{exp} repeats in HSA^{LR} mice could reverse a subset of mis-spliced RNAs.¹⁷ Using the ASO-induced RNA cleavage strategy, the same group showed that targeting the chimeric actin gene in HSA^{LR} mice could correct myotonia and also that targeting the *DMPK* gene was possible following systemic injections in asymptomatic DM1 mice.¹⁸ We hypothesized the reduction in the level of mutant transcripts by targeting the *DMPK* transcript with an ASO-inducing RNA cleavage would alleviate pathological phenotypic traits in a mouse model of DM1, such as the loss of strength. We recently identified two ASOs, a 2'-4'-constrained ethyl (cEt) and a 2'-O-methoxyethyl (MOE) gapmers, which were able to achieve strong

Received 27 October 2016; accepted 10 May 2017;
<http://dx.doi.org/10.1016/j.omtn.2017.05.007>

Correspondence: Jack Puymirat, Laval University Experimental Organogenesis Center/LOEX, Enfant-Jésus Hospital, 1401, 18^e Rue, Québec, QC, G1J 1Z4, Canada.
E-mail: jack.puymirat@crchudequebec.ulaval.ca

knockdown of *DMPK* mutant transcripts in DM1 cells and in a mouse model of DM1.^{18,19}

RESULTS

ISIS 445569 and ISIS 486178 Reduce *DMPK* mRNA Levels in Human DM1 Muscle Satellite Cells

Over 3,000 ASOs containing either MOE, cEt, or a combination of both chemistries were previously screened for inhibition of human *DMPK* expression.¹⁹ We identified two ASOs, the first bearing MOE modifications complementary to a region in exon 15 upstream to the (CUG)_n repeats within the 3' UTR of *DMPK*, and the second bearing cEt modifications complementary to a region in exon 15 downstream to the aforementioned (CUG)_n repeat, which exhibited particularly high potency (Figure 1A). ISIS 445569 and ISIS 486178 are 100% complementary to human *DMPK* gene; however, ISIS 486178 is also 100% complementary to the monkey and mouse *Dmpk* gene. Human DM1 muscle satellite cells were transfected with different concentrations (1, 5, 10, 20, 50, 125, 250, 500, and 1,000 nM) of each oligonucleotide in the presence of Lipofectamine 2000 transfection reagent (Invitrogen). Blind analysis for RNA foci was performed after 2 days of differentiation. Quantification of nuclear foci, as identified by fluorescence in situ hybridization (FISH), revealed a dose-dependent disappearance of nuclear foci (Figure 1B) in human DM1 myotubes, with a maximum effect (>90% of foci disappearance; Figure 1C) occurring at 20 nM for both ASOs (Figure S1). Northern blot analysis confirmed that both ASOs induced a 90% reduction of the mutant transcripts (Figures 1D and 1E). As expected, because both ASOs were not specific for the mutant transcripts, a 70% reduction of the wild-type *DMPK* transcripts was also observed. Nuclear redistribution of *MBNL1* also occurred after treatment with both ASOs (Figure S2), indicating that CUG^{exp} repeats are effectively degraded after cleavage events at either the 5' or 3' side of the repeat tract at the site targeted by the respective ASOs.

In a previous study, we identified a set of mis-spliced RNAs present in human DM1 muscle satellite cell cultures²⁰ that can be used to monitor alternative splicing corrections 48 hr after transfection. Treatment of DM1 cells with both ASOs consistently corrected the mis-splicing of *SORBS1*, *CAMK2G*, *DMD*, *PDLIM3*, and *TTN* transcripts (Figure 1F).

ISIS 445569 and ISIS 486178 Are Well Tolerated in Normal Myotubes

In order to assess the potential cellular toxicity of the two ASOs under study, a microarray was performed in normal myotubes treated with these ASOs at ten times their optimal concentration. Using gene ontology (GO) assignments to categorize genes for their involvement in apoptosis, cytotoxicity, and inflammation processes, no genes assigned to these GO categories were significantly affected (i.e., by a change ≥ 2 -fold). Other genes affected by ISIS 486178 are listed in Table S1. Moreover, we performed a cell apoptosis and necrosis assay (Figure S3) and were unable to detect any significant cell-death-associated event. Therefore, ISIS 445569 and ISIS 486178 appeared to display efficacy and tolerability in cell culture, supporting advancing into in vivo studies.

Systemic Administration of ISIS 445569 and ISIS 486178 Reduce *DMPK* mRNA Levels in DMSXL Mice

On the basis of previous data, experimental procedures were done in homozygous female mice rather than in males because muscle function analysis was more consistent.¹⁵ We evaluated these two ASOs in homozygous DMSXL mice by subcutaneous (s.c.) injection of 25 mg/kg (ISIS 486178) and 50 mg/kg (ISIS 445569) of ASO biweekly for the first 4 weeks, and then once a week for the following 5 weeks. Dosage was chosen based on dose-response experiments previously performed in heterozygous DMSXL mice.¹⁹ After 9 weeks of administration (13 injections), ASOs reduced the number of nuclear foci by 70% and 40% in the quadriceps (Figures 2A and S4) for ISIS 486178 and ISIS 445569, respectively. Furthermore, RT-qPCR confirmed these numbers, with an average of 66% (ISIS 486178) and 41% (ISIS 445569) reduction in human mutant DM1 transcripts in six skeletal muscles (tibialis anterior, soleus, quadriceps, latissimus dorsi, triceps, and diaphragm) (Figure 2B). Only ISIS 486178 had an effect in the heart, with a 31% decrease in mutant transcripts, and no significant decrease was observed in the brain with either ASO, as expected based on poor blood-brain barrier penetration of ASOs.²¹ These data indicate that the cEt-containing *DMPK* ASO ISIS 486178 is more efficient than the MOE ASO ISIS 445569 for targeting mutant transcripts in muscle tissues after systemic injection.

ISIS 486178 Increases Body Weight in DMSXL Mice

We have previously shown that homozygous DMSXL female mice have a reduced body weight compared to age-matched wild-type mice.¹⁵ To determine whether the decrease in CUG^{exp} RNAs by ASOs attenuate this loss in body weight, DMSXL mice were treated with 25 mg/kg of ISIS 486178 twice a week for 4 weeks. A significant increase in body weight was observed after 4 weeks of treatment ($p = 0.016$). On the other hand, no significant effect was observed with the less potent ASO ISIS 445569 (Table 1).

ISIS 486178 Increases Muscle Strength in DMSXL Mice

Ideally, a therapeutic reduction of CUG^{exp} RNAs would lead to increased muscle strength in the DMSXL mice. We have previously shown that these mice exhibit a 30% reduction in forelimb strength compared to age-matched wild-type mice using the grip test.¹⁵ During the 2-month treatment period, untreated homozygous DMSXL mice lost 5.9 g in force, whereas treatment with ASO ISIS 486178 significantly increased muscle strength by 2.6 g ($p = 0.003$). A partial improvement of 0.5 g was seen following ISIS 445569 treatment, but was not significant when compared to average force variation in the DXSXL mice (Figure 2C). As in a previous characterization of these mice,¹⁵ the correlation between strength phenotype and specific force was not possible (data not shown).

ISIS 486178 ASO Treatment Improves Skeletal Muscle Maturation in DMSXL Mice

Studies on rat soleus muscle development revealed an early muscle fiber distribution, with mixed fibers type 1/2a (2c) transitioning to type 1 after a few months of life.²² Four-month-old DMSXL mice have been reported to exhibit a higher proportion of fibers 1/2a in soleus

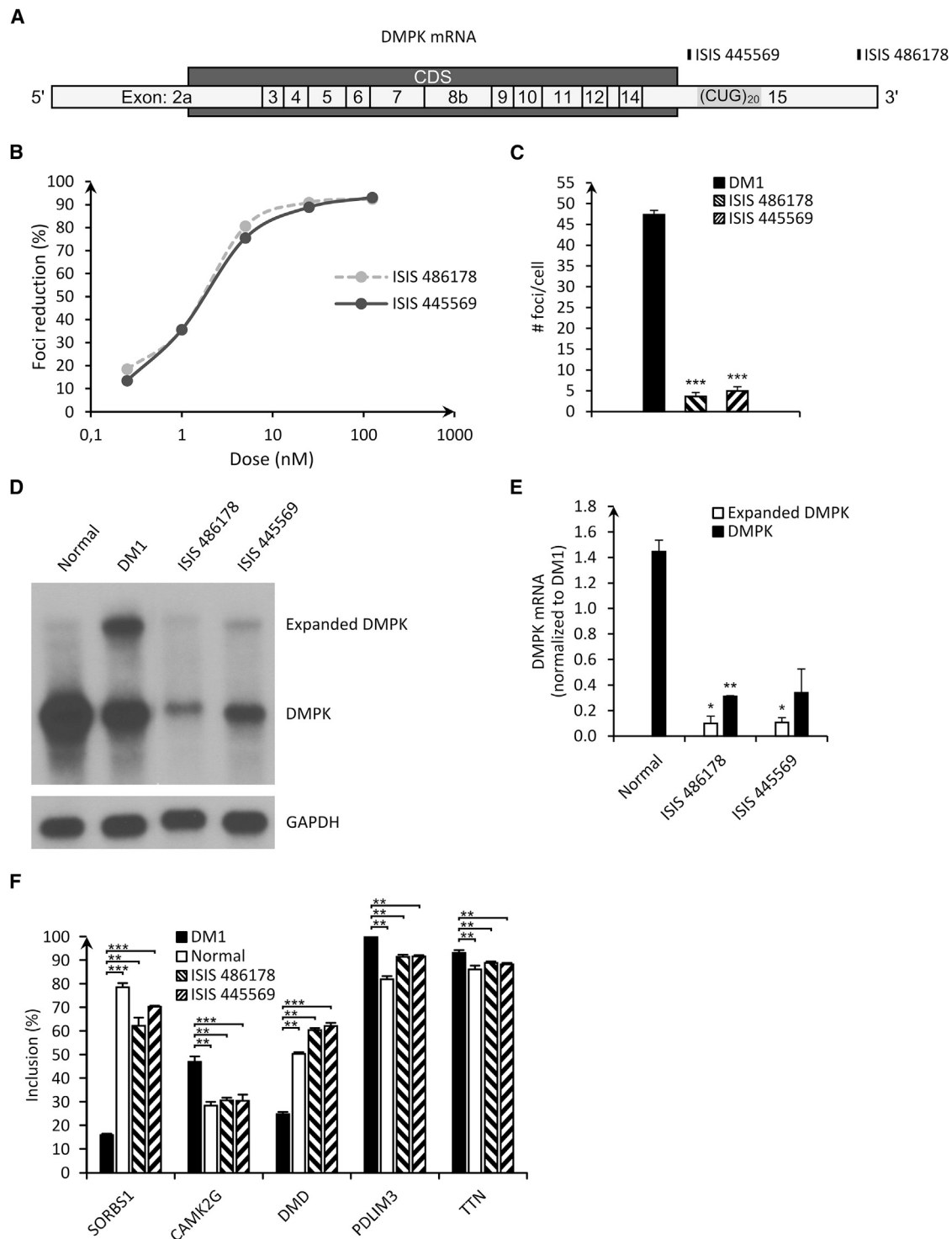


Figure 1. In Vitro Evaluation of ISIS 486178 and ISIS 445569 ASOs in DM1 Muscle Satellite Cells

(A) ASO targets on exon 15 of the *DMPK* mRNA transcript variant 1 (GenBank: NM_001081563). (B) Dose effect curves of ISIS 486178 and ISIS 445569 ASOs estimated by foci reduction in myotubes (n = 10). (C) FISH quantification of foci per nucleus reduction by ASO treatment in DM3200 myotubes (n = 6). (D) Northern blot shows expanded and normal *DMPK* mRNA after treatment by ASOs. Probes were hybridized and revealed one at a time on the same membrane. (E) Quantification of the reduction of *DMPK* mRNA from northern blot autoradiograms (n = 2). (F) Inclusion of mis-spliced events *SORBS1*, *CAMK2G*, *DMD*, *PDLIM3*, and *TTN* (n = 3). *p < 0.05; **p < 0.01; ***p < 0.001 by unpaired two-tailed t test.

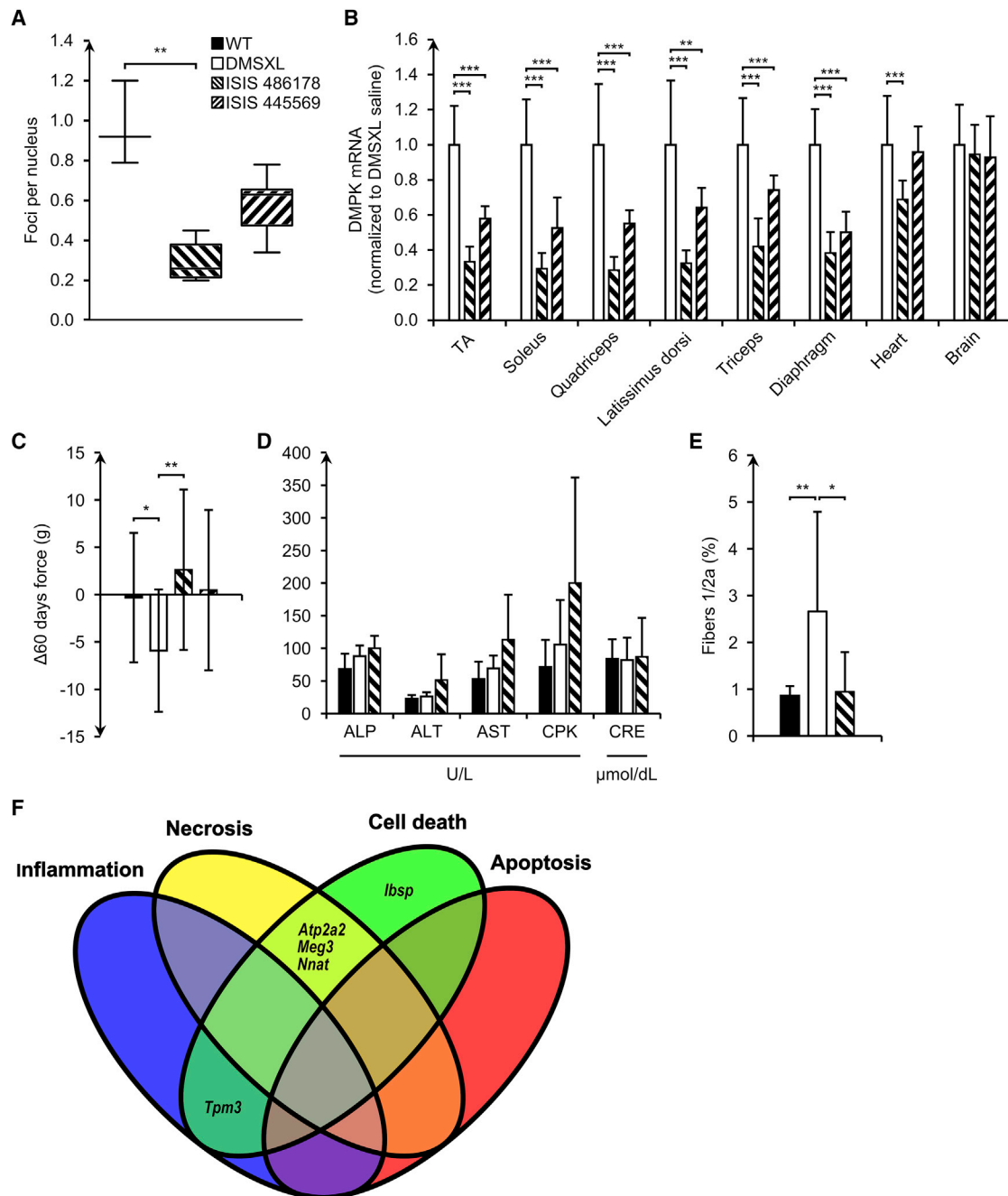


Figure 2. Evaluation of ISIS 486178 and ISIS 445569 ASOs upon Systemic Administration in DMSXL Mouse

(A) FISH quantification of foci per nucleus in DMSXL mice quadriceps ($n = 3$; treated $n = 9$ per ASO; multiple sections throughout the muscle for each mice). $**p < 0.01$ by Kruskal Wallis test. (B) *DMPK* mRNA in transgenic DMSXL mice treated with ISIS 486178 (25 mg/kg) and ISIS 445569 (50 mg/kg) (DMSXL, $n = 11$; ISIS 486178, $n = 17$; 445569, $n = 7$). (C) Mice forelimb strength after treatment with by ASOs (wild-type [WT], $n = 24$; DMSXL, $n = 15$; ISIS 486178, $n = 15$; ISIS 445569, $n = 7$). (D) DMSXL mice serum chemistry after ISIS 486178 injection regimen. (E) Muscle fibers type 1/2a in mice soleus (WT, $n = 3$; DMSXL, $n = 12$; ISIS 486178, $n = 5$; ~4,500 fibers/mouse). (F) Cell death, necrosis, and inflammation genes downregulated by a 2-fold change in DMSXL mice treated with ISIS 486178 determined by microarray ($n = 6$). $*p < 0.05$; $**p < 0.01$; $***p < 0.001$ by unpaired two-tailed t test.

Table 1. Body Weight in Female DMSXL Mice Treated for 2 Months with ASOs

Mean Body Weight (g) ± SD					
	Day 0	Day 30	Day 60	Δ60	p Value
DMSXL	18.1 ± 1.9	18.4 ± 1.8	18.2 ± 2.4	0.1	0.5
ISIS 486178	17.2 ± 1.9	18.3 ± 1.6	18.7 ± 1.7	1.5	0.016
ISIS 445569	17.4 ± 1.5	18.2 ± 2.0	18.4 ± 3.1	1.0	0.2
Wild-type	22.8 ± 1.6	23.9 ± 1.2	23.8 ± 1.7	1.7	0.06

(n = 10; ISIS 445569, n = 8) p values by unpaired two-tailed t test.

muscle than have age-matched wild-type mice,¹⁵ which might be linked to delayed muscle fiber differentiation, as found in CDM1 patients.² This prompted us to investigate the possibility of reversing the persistent fiber immaturity profile following treatment with ASOs. Immunostaining of soleus muscle fibers, which express both myosin heavy chain 1 and 2a in 7-month-old homozygous DMSXL revealed a 2.7% abundance of type 1/2a fibers, whereas only 0.85% of these fibers can be observed in age-matched wild-type mice. Treatment of DMSXL mice with ASO ISIS 486178 restored 95% of the normal profile of type 1/2a fibers in DMSXL mice (Figure 2E).

ISIS 486178 ASO Treatment Causes No Overt Toxicity in DMSXL Mice

Treatment of DMSXL mice with ISIS 486178 and ISIS 445569 for 9 weeks was not associated with any mortality. One untreated DMSXL mouse died a few hours prior to necropsy, and another died before the first injection. No DMSXL mice treated with ASO ISIS 486178 and ISIS 445569 died during the experiment. No liver anomalies were visually detected during necropsy, whereas alkaline phosphatase (ALP), alanine transaminase (ALT), and aspartate transaminase (AST) blood levels all remained within normal limits, without any significant variation (Figure 2D). Likewise, creatine kinase (CPK) and creatinine (CRE) levels, which are markers for tissue and kidney damage, respectively, were shown to stay within the normal thresholds for the course of the experiment.

A microarray on tibialis anterior muscle samples from ISIS-486178-treated DMSXL mice provided a good opportunity to examine its effect on the expression inflammation, necrosis, apoptosis, and other cell death genes using GO analysis. Only five endogenous genes were found to be downregulated by treatment (i.e., by ≥ 2 -fold change; Table S2), namely *Ibsp*, *Atp2a2*, *Meg3*, *Nnat*, and *Tpm3* (Figure 2F). The microarray also corroborated our RT-qPCR results for *Dmpk* gene expression, with a 73% reduction.

Evaluation of ISIS 486178 ASO Treatment in Wild-Type Mice

Because the ISIS 486178 sequence also targets the endogenous mouse *Dmpk* transcripts, we next analyzed its effect in wild-type mice following s.c. injection. After 9 weeks of administration, a strong decrease in endogenous *Dmpk* mRNA was detected (Figure S5). Despite the strong downregulation of *Dmpk* expression, no significant

changes in growth, mortality, or muscle strength were detectable after treatment (data not shown). These results indicate that the decrease in endogenous *Dmpk* mRNA by ISIS 486178 had no effect on the *DM1* phenotype, in good agreement with our previous data¹⁹ and with data showing that knockout of the *Dmpk* gene in transgenic mice induce only a late-onset progressive myopathy.²³ The latter observations suggest that the residual *Dmpk* mRNA levels might be sufficient to counteract these effects and sustain normal function.

DISCUSSION

Homozygous DMSXL mice display high mortality during the first month of life, as well as growth retardation, decrease in muscle strength, motor performance, and cognitive impairments, but no or only mild myotonia.¹⁶ Histological features of the skeletal muscles revealed a decrease in the mean muscle fiber cross-sectional area, an increase in the number of oxidative fibers, and an increase in mixed fibers 1/2a, which may point to a potential delay in muscle maturation. The clinical and histological manifestations observed in DMSXL mice are characteristically closer to those observed in the congenital rather than the adult form of the disease. The absence of the classical histological features observed in human DM1 skeletal muscle, such as type 1 fiber atrophy and type 2 fiber hypertrophy, ringed fibers, sarcoplasmic mass, and mild splicing abnormalities are also consistent with this observation.¹ There is indeed a lack of data for the involvement of the spliceopathy in the pathogenesis of the congenital form of the disease. Very mild and variable mis-splicings have been characterized in DMSXL mice¹⁵ but did not prove to represent a significant measure of pathological outcome in this model for ASO screening. Insertional effects in DMSXL mice can be ruled out because parental homozygous mice carrying 500–600 repeats (DM300) have very mild or no detectable phenotype.^{15,24,25} Short-term therapy with ASOs produced a sustained phenotypic disease reversal, including gain of body weight, increase in muscle strength, and restoration in skeletal muscle maturation. These results show that muscle weakness in DM1 can be improved using a targeted approach to eliminate toxic RNAs. This indicates that muscle weakness may be reversible in a DM1 patient.

In this report, we demonstrate that a cEt-modified ASO (ISIS 486178) targeting *DMPK* mRNA significantly reduced mutant transcripts in cells and generates a reproducible and robust reduction in skeletal muscle *DMPK* mRNAs in DM1 mice following s.c. administration. The MOE gapmer ASOs have been shown to reduce mutant *DMPK* transcripts in the skeletal muscles of DMSXL mice following s.c. administration, but at higher doses than those required for the cEt-modified ASOs. A 50% and 75% reduction in *DMPK* RNAs were observed in skeletal muscles at 50 and 75 mg/kg, respectively, twice a week for 4 weeks using MOE gapmer ASOs.¹⁸ The potent activity of cEt-modified oligonucleotides in skeletal muscle has also been demonstrated for an androgen receptor (AR) targeting ASO in AR transgenic mice.²⁶ Activity in skeletal muscle has also been described for a peptide-PMO conjugate, Pip5e-PMO, with a single dose of 12–25 mg/kg and showed highly efficient exon skipping and dystrophin production in mdx mice, with >80% dystrophin-positive

fibers measured in all skeletal muscle groups after systemic injection.²⁷ In contrast with what was observed with the cEt-modified ASO in DMSXL mice, no phenotypic reversion was observed following systemic injection of 12 mg/kg Pip6a-PMO (more efficient peptide ASO than Pip5e-PMO) likely due to uncompromised muscle cell membranes in DMSXL mice (J. Puymirat, unpublished data). The difference between the dose of ASOs used in mdx and DMSXL mice may be explained by more than one factor. The physical chemical behavior of the neutral PMO to the negatively charged cEt ASO will affect cell intake. Second, there is the matter of the cell-penetrating peptide attached to the PMO, which may improve cell penetration. Lastly, it has been shown that the muscle membrane is more permeable in mdx but not DMSXL mice,²⁸ which may facilitate ASO delivery following systemic administration.

The design used for the cEt-modified ASO is an interesting tool to modulate genes in skeletal muscle upon systemic administration. The decrease of only 30% of *DMPK* transcripts found in the heart after systemic administration suggests that the delivery of ISIS 486178 displays tissue specificity. It is of note, however, that DM1 transcripts could be reduced by as much as 60% in the heart using a dose of 100 mg/kg/week.¹⁹ Our data agree with previously published tissue distribution of cEt-gapmer ASO using a pan-oligonucleotide antibody.²⁹ The inability of ISIS 486178 to effectively cross the blood-brain barrier indicates that other delivery methods will have to be considered for the treatment of DM1-related cognitive impairments. To this end, intraventricular administration in mice could potentially resolve this issue³⁰ and needs further investigation. In humans, intrathecal administration of the SPINRAZA ASO, which is designed to target motor neurons in patients with infantile spinal muscular atrophy (SMA), is being commercialized,⁴⁵ showing the potential of this approach in DM1.

The cEt chemistry has been shown to be 3- to 5-fold more potent than that of the MOE-modified ASOs and is comparable to that of LNAs; however, the cEt-modified nucleoside appears to be better tolerated than LNA.³² Neither overt nor new toxicity was found to be associated with their use, in agreement with a previous report showing that the toxicity profile of cEt ASOs is very similar to that of MOE ASOs in mice and monkeys.²⁹ The 3-10-3 gapmer design also contributes to the low hepatotoxicity by the limited amount of high-affinity modified nucleosides, which reduces high-affinity-induced imperfect hybridizations and, therefore, RNase H1-dependent non-specific toxicity.³³ In parallel to this study, a full toxicity evaluation of ASO ISIS 486178 was conducted in a cynomolgus monkey by Ionis Pharmaceuticals and provided sufficient basis to launch a phase I/II clinical evaluation of a similar class of *DMPK* ASO, ISIS-DMPK_{Rx}. We have previously published the pharmacokinetics and pharmacodynamics for ASO ISIS 486178 in both normal mice and monkeys. The activity of the ASO was similar in wild-type mice and DMSXL mice,¹⁹ supporting that the pharmacokinetic in this mouse model is not significantly different than that in wild-type mice. Finally, we present a preclinical evaluation of a gene therapy for DM1 based on the elimination of toxic RNAs.

cEt gapmer ASO chemistry opens new avenues for the development of gene therapies based on gene silencing for several muscular dystrophies, such as DM1.

This study provides evidence that muscle strength can be improved following elimination of toxic RNAs in patients with DM1. Further work is needed to determine the long-term effects and toxicity of ASOs, although we recently showed that the reduction of *Dmpk* RNA levels in muscle was maintained for up to 16 and 26 weeks post-treatment in mice and monkeys, respectively,¹⁹ suggesting that these ASOs may be effective in the long term. This is in good agreement with a previous study showing that treatment of a DM1 mouse model with MOE ASO results in an improvement of symptoms for up to 12 months after discontinuation of treatment.¹⁸ The long-term beneficial effect of ASO treatment is also in agreement with other studies showing the long-term usefulness of chemically modified ASO therapy for the treatment of liver diseases³⁴ and hypercholesterolemia.^{35,36}

MATERIALS AND METHODS

Antisense Oligonucleotides

Synthesis³¹ and identification¹⁹ of active ASOs was performed by Ionis Pharmaceuticals, as previously described, and blinded for our evaluation. The design included a central gap region of ten DNA nucleotides with either a MOE or cEt modification at both ends, with phosphorothioate for intersubunit linkage. ISIS 445569 is a 5-10-5 MOE gapmer with sequence 5'-CGGAGCGGTTGT GAACTGGC-3'¹⁸ and ISIS 486178 is a 3-10-3 cEt gapmer with sequence 5'-ACAATAAATACCGAGG-3'.

Cell Culture and Transfection

Human fetal normal and congenital fetal DM1 (carrying 3,200 repeats) muscle satellite cells, which were previously described,³⁷ were grown in MB-1 medium (Thermo Scientific) supplemented with BSA 0.5 mg/ml (Sigma-Aldrich), insulin 5 µg/ml (Sigma-Aldrich), and dexamethasone 0.4 µg/ml (Sigma-Aldrich). Cells were transfected at 80% confluence, with ASOs ranging from 1 nM to 1 µM, using Lipofectamine 2000 reagent (Invitrogen), according to the manufacturer's instructions. Differentiation into myotubes was obtained by switching cultures to differentiation medium (DMEM high glucose [Life Technologies] supplemented with 2% horse serum [Invitrogen], 10 µg/ml insulin [Sigma-Aldrich], and 100 µg/ml apo-transferrin [Sigma-Aldrich]) 24 hr after transfection, and analysis was performed after 2 days. Apoptosis and necrosis assays were carried out in proliferating human fetal normal cells using an Annexin V-FITC Apoptosis Kit (PromoKine) per manufacturer's instructions and quantified by flow cytometry using a BD FACSCanto II (BD Biosciences).

Northern Blot Analysis

RNA was prepared by lysing 10 million cells in 2 mL of proteinase K solution (500 µg/ml proteinase K [QIAGEN]; 200 mM NaCl [Fisher Scientific]; 200 mM Tris-HCL, pH 7.5 [Wisent]; 1.5 mM MgCl₂ [Fisher Scientific]; and 2% SDS [Roche]) for 30 min at 55°C. mRNA was then isolated with 60 mg of oligo(dT) (Sigma-Aldrich)

using microcentrifuge spin columns (Ambion). Concentrated mRNA was quantified by absorbance at 260 nm on a NanoDrop 2000c (Thermo Scientific), and quality was verified on an agarose gel by controlling residual 28S/18S contamination. 3 µg of mRNA were separated on a 1% agarose gel containing MOPS (Laboratoire MAT) and 0.62 M formaldehyde (Sigma-Aldrich) and transferred to Immobilon-NY+ nylon membrane (Millipore) by downward alkaline blotting and hybridized with human ³²P-labeled *DMPK* or *GAPDH* oligonucleotide probes. Probes were generated by random priming (New England Biolabs) of 100 ng of *DMPK* cDNA fragments (BglII-SacI) or *GAPDH* cDNA PCR-amplified fragments (Table S3). Overnight hybridization was conducted at 65°C in hybridization buffer (1X SSPE [Sigma]; 2X Denhardt's [Sigma]; 10% dextran sulfate [Fisher Scientific]; 1% SDS [Roche]; 100 µg/mL salmon sperm DNA [Ambion]; and probe 1 Mcpm/mL). Relative quantification of mRNA levels on scanned autoradiograms (600 dpi) was determined by densitometry using ImageJ 1.47 software.

Immunostaining - FISH

Cells grown on gelatin-coated coverslips were fixed with pre-chilled 50% acetone/50% methanol (Fisher Scientific) for 5 min at -20°C. After blocking with 3% BSA (Sigma), coverslips were incubated at 37°C for 1 hr with MB1a(4A8) (MDA Monoclonal Antibody Resource)³⁸ mouse monoclonal immunoglobulin G1 (IgG1) antibody against *MBNL1* (one-fourth in 1X PBS/3% BSA). Secondary antibody Alexa Fluor-488 goat α-mouse IgG (H+L) (Molecular Probes) was used at 4 µg/mL, followed by a 1-hr incubation at 37°C. Sense ribonuclear inclusions were detected intracellularly with a 5'-Cy3-labeled (CAG)₅ PNA probe (PNA Bio). Immunostaining was followed by 4% formaldehyde (Sigma-Aldrich) fixation and incubated for 20 hr at 37°C in hybridization buffer (1 µg/µL *E. coli* tRNA [Sigma-Aldrich]; 5% dextran sulfate [Fisher Scientific]; 0.02% BSA [Sigma-Aldrich]; 2X SSC [Sigma-Aldrich]; 50% formamide [Fisher Scientific]; 2 mM vanadyl ribonucleoside complex [Sigma-Aldrich]; and 1 ng/µL PNA probe). The coverslips were washed twice in 2X SSC (Sigma)/50% formamide (Fisher Scientific) for 30 min at 37°C, stained with 5 µM DRAQ5 (Thermo Scientific) for nucleus visualization, mounted on slides with Fluoromount (Sigma), and sealed with generic clear nail polish. Cells were examined under a FluoView 300 confocal microscope (Olympus) using argon-ion 488-nm, He-Ne 543-nm, and He-Ne 633-nm lasers. Filters used were BA510IF + BA530RIF (green), 605BP (red), and BA660IF (far-red), with a PlanApo 60X/1.4 oil ∞/0.17 objective. Quantification of FISH was performed using ImageJ 1.47 software.

Quadriceps sense ribonuclear inclusions were detected on 10-µm-thick transverse serial sections with a 5'-Cy3-labeled (CAG)₅ RNA probe (Sigma). Thawed cross-sections were fixed in 4% buffered formaldehyde (Microm Microtech) during 20 min and permeabilized in 1X PBS (Sigma)/2% acetone (Fisher Scientific) for 5 min. Using Discovery Ventana Automaton (Roche), as previously described,³⁹ sections were incubated for 7 hr at 44°C with the probe in RiboHybe reagent (Roche), then counterstained with Hoechst 14533 (Sigma) and mounted with VECTASHIELD H-1000 (Vector) mounting me-

dium. Slide observations were performed using an Axioplan 2 Imaging microscope (Zeiss). Four transverse levels of every quadriceps specimen were studied. Each cryosection was randomly subdivided into three areas to assess nuclear foci-containing cells up to an observation threshold for positivity of >100 nuclei in each cryosection. Image acquisitions were performed using an LSM 510 Meta confocal microscope (Zeiss) and were composed using ImageJ 1.41 software.

Study Approval

All animal experiments were approved by the Institutional Animal Care and Use Committees at the CRCHU de Québec and Ionis Pharmaceuticals.

Experimental Mice

DMSXL mice carry a 45-kb human genomic fragment that includes the mutant *DMPK* gene with 1,000-1,600 CTG repeats. The homozygous DMSXL mice display several features of DM1, such as high neonatal mortality, growth delay, mis-spliced preRNAs, decrease in muscle strength, and histological changes. Experiments were carried out on 2- to 4-month-old homozygous mice, an age at which the phenotype is well characterized.¹⁵

Subcutaneous Injection of ASOs

All ASOs were dissolved in PBS. Doses of 25 mg/kg (ISIS 486178) or 50 mg/kg (ISIS 445569) were injected s.c. twice a week in the interscapular region for 4 weeks and then once a week for an additional 5-week interval. The doses used were selected based on preliminary dose-response experiments in heterozygous DMSXL mice. Injection volumes ranged from 50 to 250 µL.

Blood Chemistry

Mice blood was collected by cardiac puncture, transferred to serum separator tubes (BD Bioscience), left for 30 min at room temperature for coagulation, and centrifuged at 2,000 × g for 15 min. Serum was transferred to new tubes and kept at -20° until analysis. Plasma serum AST, ALT, CRE, CPK, and ALP were determined using Olympus reagents and an Olympus AU400e analyzer.

Real-Time qPCR Assay

Total RNA was purified from mouse tibialis anterior, soleus, triceps, quadriceps, latissimus dorsi, diaphragm, heart, and brain after flash freezing in liquid nitrogen. The isolation process started with a crude homogenization of 25 mg of tissue in proteinase K solution (10 mM Tris-Cl, pH 7.5 [Wisent]; 10 mM EDTA [Sigma-Aldrich]; 2% SDS [Roche]; 500 mM NaCl [Fisher Scientific]; 1.5 mM MgCl₂ [Fisher Scientific]; and 500 µg/mL proteinase K [QIAGEN]), followed by complete homogenization with a TissueLyser LT (QIAGEN) using a ball bearing. After a 30-min incubation at 55°C, standard QIAzol (QIAGEN) protocol for tissue extraction was performed along with RNA quantification with a NanoDrop 2000c (Thermo Scientific), and RNA integrity was verified on a 2100 Bioanalyzer (Agilent Technologies). cDNA was then produced using Quantitect Reverse Transcription (QIAGEN) on 200 ng of RNA, and RT-qPCR was used to determine mRNA levels for *DMPK* and *Dmpk* mRNA, with *Hprt1*,

Rpl13a, and *Tbp* RNAs as normalization controls (primers in Table S3) on a LightCycler 480 II (Roche) using SYBR Green I Master hot start reaction mix.

RT-PCR Analysis of Alternative Splicing

The design of primer sets and targets for SORBS1, CAMK2G, DMD, PDLIM3, and TTN mis-spliced events were previously described (primers in Table S3).²⁰ Total RNA was extracted using QIAzol (QIAGEN) and quantified with a NanoDrop 2000c (Thermo Scientific), and the RNA integrity was verified with a 2100 Bioanalyzer (Agilent Technologies). A total of 400 ng of RNA was reverse transcribed using a QuantiTect Reverse Transcription kit (QIAGEN) in a final volume of 20 μ L. 1 μ L of cDNA was amplified with 2.5 U/50 μ L of HotStarTaq Plus DNA Polymerase (QIAGEN) in the buffer provided by the manufacturer in the presence of the specific primers (IDT; 250 nM) for each splicing and 200 μ M desoxynucleotide triphosphates (dNTPs) (Thermo Scientific). A first cycle of 5 min at 95°C was followed by 40 cycles of 30 s at 94°C, 30 s at 55°C, and 30 s at 72°C. Thermocycling ended with an extension step of 10 min at 72°C. Visualization of the amplified products was performed on Tris-borate-EDTA (TBE) 1.5% agarose multipurpose (MP) gels (Roche) using GelRed nucleic acid stain (Biotium), and analysis was carried out by densitometry using ImageJ 1.47 from gel pictures taken with an AlphaImager (Alpha Innotech).

Transcriptome Analysis by Microarray

RNA was isolated from human fetal normal cells treated with both ASOs using QIAzol (QIAGEN). DNA microarray analyses were carried out with Affymetrix Human Gene 1.0 ST arrays (Affymetrix) according to their standard protocol. RNA from DMSXL mice treated with ISIS 486178 was isolated from tibialis anterior muscle using the proteinase K method. Six mice per condition were separated into two pooled groups for analysis. DNA microarray analyses were carried out with Affymetrix Mouse Gene 2.0 ST arrays according to the Affymetrix standard protocol. The amount of total RNA was measured using a NanoDrop ND-1000 spectrophotometer (Thermo Scientific). Optical density values at 260/280 were consistently above 1.9. Total RNA quality was assayed on an Agilent BioAnalyzer (Agilent Technologies). Briefly, 200 ng of total RNA per sample was labeled using the Affymetrix GeneChip WT cDNA Synthesis and Amplification Kit protocol and hybridized to the arrays as recommended by the manufacturer (Affymetrix). The cRNA hybridization cocktail was incubated overnight at 45°C while rotating in a hybridization oven. After 16-hr hybridization, the cocktail was removed and the arrays were washed and stained in an Affymetrix GeneChip fluidics station 450, according to the Affymetrix-recommended protocol. The arrays were scanned using the Affymetrix GCS 3000 7G and Gene-Chip Operating Software (Affymetrix) to produce the intensity files. The background subtraction and normalization of probe set intensities was performed using the method of robust multiarray analysis (RMA) described previously.⁴⁰ For Affymetrix Human Gene 1.0 ST arrays, differentially expressed genes were identified by comparison of gene expression intensity using a moderated t test, and a Bayes smoothing approach was developed for a low number of repli-

cates.⁴¹ To correct for the effect of multiple testing, the false discovery rate was estimated from *p* values derived from the moderated t test statistics.⁴² The analysis was performed using the affyGUI Graphical User Interface for the Limma microarray package⁴³ and GO analysis using the GO enrichment functionality in the Partek Genomics Suite software. For Affymetrix Mouse Gene 2.0 ST arrays, the CHP files were imported and analyzed with the Transcriptome Analysis Console Software (Affymetrix). Microarray analyses were performed by the CHU de Québec Research Center (Centre de Recherche du Centre Hospitalier Universitaire) Gene Expression Platform.

Muscle Fiber Morphometry

Frozen transverse 10- μ m serial sections of muscles were air-fixed on slides for 15 min and incubated for 1 hr in blocking solution (10% goat serum [Sigma-Aldrich]; 2% BSA [Sigma-Aldrich]; and 1X PBS [Sigma-Aldrich]) at room temperature. Sections were then incubated consecutively for 1 hr each at 37°C with two mouse monoclonal antibodies with different isotypes directed against myosin heavy chain type 1 (BA-D5, IgG2b; DSHB) and type 2a (SC-71, IgG1; DSHB). Secondary antibodies were 2.5 μ g/mL Cy3 rabbit anti-mouse IgG1 (Novus Biologicals) and 5 μ g/mL Alexa Fluor-350 goat anti-mouse IgG2b (Molecular Probes). Slides were mounted with Fluoromount (Sigma) and fixed with generic clear nail polish, and images were acquired with an Eclipse TE300 (Nikon) microscope. Counts of muscle fibers positive for type 1 and 2a myosin heavy chain were performed using ImageJ 1.47 software.

Grip Test

Mice grip strength was assessed using a Chatillon grip strength digital dynamometer (Columbus Instruments) using a previously described protocol.⁴⁴

Statistical Analysis

Statistical analyses were performed using a two-tailed unpaired Student's t test with unequal variance, and *p* < 0.05 was considered significant. Foci in DMSXL mice quadriceps were analyzed by the Kruskal Wallis test, with *p* < 0.05 being considered significant.

SUPPLEMENTAL INFORMATION

Supplemental Information includes five figures and three tables and can be found with this article online at <http://dx.doi.org/10.1016/j.omtn.2017.05.007>.

AUTHOR CONTRIBUTIONS

J.P. and C.F.B. conceived the study and provided leadership. Anti-sense screening was performed by A.R.M. and S.K.P. under supervision of C.F.B. at Ionis Pharmaceuticals, Inc., with the help of T.M.W. and C.A.T. G.G. provided the DMSXL mice as well as her expertise with their phenotype. L.R. and A.L. performed FISH on DMSXL mice tissues and automated analysis under G.B. S.K.P. performed the blood biochemistry on mice serum. J.C. assisted with animal experiments, immunostaining, and molecular biology experiments, whereas L.M. assisted with the cell culture work. D.J. participated in the experimental design, performed most of the experiments and

data analysis, and wrote the manuscript, with the assistance of J.P. and guidance of C.F.B.

CONFLICTS OF INTEREST

Partial research support was funded by Ionis Pharmaceuticals, Inc. S.K.P., A.R.M., and C.F.B. were employees of Ionis Pharmaceuticals, Inc. and inventors on patent # WO2015021457A3 regarding ISIS 486178/ISIS 445569 antisense technology for modulation of *DMPK* expression.

ACKNOWLEDGMENTS

This work was supported by Ionis Pharmaceuticals, Inc. and Muscular Dystrophy Association grant MDA417929. We acknowledge the Bioimaging platform of the Infectious Disease Research Centre, funded by equipment and infrastructure grants from the Canada Foundation for Innovation (CFI). We would also like to thank Denis Furling, who graciously provided the DM1 cell line used in this study.

REFERENCES

- Harper, P.S. (2001). Myotonic Dystrophy (Saunders).
- Farkas-Bargeton, E., Barbet, J.P., Dancea, S., Wehrle, R., Checouri, A., and Dulac, O. (1988). Immaturity of muscle fibers in the congenital form of myotonic dystrophy: its consequences and its origin. *J. Neurol. Sci.* 83, 145–159.
- Furling, D., Coiffier, L., Mouly, V., Barbet, J.P., St Guily, J.L., Taneja, K., Gourdon, G., Junien, C., and Butler-Browne, G.S. (2001). Defective satellite cells in congenital myotonic dystrophy. *Hum. Mol. Genet.* 10, 2079–2087.
- Sarnat, H.B., and Silbert, S.W. (1976). Maturational arrest of fetal muscle in neonatal myotonic dystrophy. A pathologic study of four cases. *Arch. Neurol.* 33, 466–474.
- Thornton, C.A. (2014). Myotonic dystrophy. *Neurol. Clin.* 32, 705–719.
- Taneja, K.L., McCurrach, M., Schalling, M., Housman, D., and Singer, R.H. (1995). Foci of trinucleotide repeat transcripts in nuclei of myotonic dystrophy cells and tissues. *J. Cell Biol.* 128, 995–1002.
- Kalsotra, A., Xiao, X., Ward, A.J., Castle, J.C., Johnson, J.M., Burge, C.B., and Cooper, T.A. (2008). A postnatal switch of CELF and MBNL proteins reprograms alternative splicing in the developing heart. *Proc. Natl. Acad. Sci. USA* 105, 20333–20338.
- Timchenko, N.A., Cai, Z.J., Welm, A.L., Reddy, S., Ashizawa, T., and Timchenko, L.T. (2001). RNA CUG repeats sequester CUGBP1 and alter protein levels and activity of CUGBP1. *J. Biol. Chem.* 276, 7820–7826.
- Paul, S., Dansithong, W., Kim, D., Rossi, J., Webster, N.J., Comai, L., and Reddy, S. (2006). Interaction of muscleblind, CUG-BP1 and hnRNP H proteins in DM1-associated aberrant IR splicing. *EMBO J.* 25, 4271–4283.
- Mankodi, A., Lin, X., Blaxall, B.C., Swanson, M.S., and Thornton, C.A. (2005). Nuclear RNA foci in the heart in myotonic dystrophy. *Circ. Res.* 97, 1152–1155.
- Kuyumcu-Martinez, N.M., Wang, G.S., and Cooper, T.A. (2007). Increased steady-state levels of CUGBP1 in myotonic dystrophy I are due to PKC-mediated hyperphosphorylation. *Mol. Cell* 28, 68–78.
- Kuyumcu-Martinez, N.M., and Cooper, T.A. (2006). Misregulation of alternative splicing causes pathogenesis in myotonic dystrophy. *Prog. Mol. Subcell. Biol.* 44, 133–159.
- Mankodi, A., Logigian, E., Callahan, L., McClain, C., White, R., Henderson, D., Krym, M., and Thornton, C.A. (2000). Myotonic dystrophy in transgenic mice expressing an expanded CUG repeat. *Science* 289, 1769–1773.
- Ho, T.H., Bundman, D., Armstrong, D.L., and Cooper, T.A. (2005). Transgenic mice expressing CUG-BP1 reproduce splicing mis-regulation observed in myotonic dystrophy. *Hum. Mol. Genet.* 14, 1539–1547.
- Huguet, A., Medja, F., Nicole, A., Vignaud, A., Guiraud-Dogan, C., Ferry, A., Decostre, V., Hogrel, J.Y., Metzger, F., Hoeflich, A., et al. (2012). Molecular, physiological, and motor performance defects in DMSXL mice carrying >1,000 CTG repeats from the human DM1 locus. *PLoS Genet.* 8, e1003043.
- Hernández-Hernández, O., Guiraud-Dogan, C., Sicot, G., Huguet, A., Lullier, S., Steidl, E., Saenger, S., Marciniak, E., Obriot, H., Chevarin, C., et al. (2013). Myotonic dystrophy CTG expansion affects synaptic vesicle proteins, neurotransmission and mouse behaviour. *Brain* 136, 957–970.
- Wheeler, T.M., Sobczak, K., Lueck, J.D., Osborne, R.J., Lin, X., Dirksen, R.T., and Thornton, C.A. (2009). Reversal of RNA dominance by displacement of protein sequestered on triplet repeat RNA. *Science* 325, 336–339.
- Wheeler, T.M., Leger, A.J., Pandey, S.K., MacLeod, A.R., Nakamori, M., Cheng, S.H., Wentworth, B.M., Bennett, C.F., and Thornton, C.A. (2012). Targeting nuclear RNA for in vivo correction of myotonic dystrophy. *Nature* 488, 111–115.
- Pandey, S.K., Wheeler, T.M., Justice, S.L., Kim, A., Younis, H.S., Gattis, D., Jauvin, D., Puymirat, J., Swayze, E.E., Freier, S.M., et al. (2015). Identification and characterization of modified antisense oligonucleotides targeting DMPK in mice and nonhuman primates for the treatment of myotonic dystrophy type 1. *J. Pharmacol. Exp. Ther.* 355, 329–340.
- Klinck, R., Fourrier, A., Thibault, P., Toutant, J., Durand, M., Lapointe, E., Caillet-Boudin, M.L., Sergeant, N., Gourdon, G., Meola, G., et al. (2014). RBFox1 cooperates with MBNL1 to control splicing in muscle, including events altered in myotonic dystrophy type 1. *PLoS ONE* 9, e107324.
- Geary, R.S., Yu, R.Z., Watanabe, T., Henry, S.P., Hardee, G.E., Chappell, A., Matson, J., Sasmor, H., Cummins, L., and Levin, A.A. (2003). Pharmacokinetics of a tumor necrosis factor- α phosphorothioate 2'-O-(2-methoxyethyl) modified antisense oligonucleotide: comparison across species. *Drug Metab. Dispos.* 31, 1419–1428.
- Ansved, T., and Larsson, L. (1989). Effects of ageing on enzyme-histochemical, morphometrical and contractile properties of the soleus muscle in the rat. *J. Neurol. Sci.* 93, 105–124.
- Reddy, S., Smith, D.B., Rich, M.M., Lefterovich, J.M., Reilly, P., Davis, B.M., Tran, K., Rayburn, H., Bronson, R., Cros, D., et al. (1996). Mice lacking the myotonic dystrophy protein kinase develop a late onset progressive myopathy. *Nat. Genet.* 13, 325–335.
- Sezner, H., Agbulut, O., Sergeant, N., Savouret, C., Ghestem, A., Tabti, N., Willer, J.C., Ourth, L., Duros, C., Brisson, E., et al. (2001). Mice transgenic for the human myotonic dystrophy region with expanded CTG repeats display muscular and brain abnormalities. *Hum. Mol. Genet.* 10, 2717–2726.
- Panaite, P.A., Kiehl, M., Kraftsik, R., Gourdon, G., Kuntzer, T., and Barakat-Walter, I. (2011). Peripheral neuropathy is linked to a severe form of myotonic dystrophy in transgenic mice. *J. Neuropathol. Exp. Neurol.* 70, 678–685.
- Lieberman, A.P., Yu, Z., Murray, S., Peralta, R., Low, A., Guo, S., Yu, X.X., Cortes, C.J., Bennett, C.F., Monia, B.P., et al. (2014). Peripheral androgen receptor gene suppression rescues disease in mouse models of spinal and bulbar muscular atrophy. *Cell Rep.* 7, 774–784.
- Yin, H., Saleh, A.F., Betts, C., Camelliti, P., Seow, Y., Ashraf, S., Arzumanov, A., Hammond, S., Merritt, T., Gait, M.J., et al. (2011). Pip5 transduction peptides direct high efficiency oligonucleotide-mediated dystrophin exon skipping in heart and phenotypic correction in mdx mice. *Mol. Ther.* 19, 1295–1303.
- González-Barriga, A., Kranzen, J., Croes, H.J., Bijl, S., van den Broek, W.J., van Kessel, I.D., van Engelen, B.G., van Deutekom, J.C., Wieringa, B., Mulders, S.A., et al. (2015). Cell membrane integrity in myotonic dystrophy type 1: implications for therapy. *PLoS ONE* 10, e0121556.
- Burel, S.A., Han, S.R., Lee, H.S., Norris, D.A., Lee, B.S., Machemer, T., Park, S.Y., Zhou, T., He, G., Kim, Y., et al. (2013). Preclinical evaluation of the toxicological effects of a novel constrained ethyl modified antisense compound targeting signal transducer and activator of transcription 3 in mice and cynomolgus monkeys. *Nucleic Acid Ther.* 23, 213–227.
- Cheng, H.M., Chern, Y., Chen, I.H., Liu, C.R., Li, S.H., Chun, S.J., Rigo, F., Bennett, C.F., Deng, N., Feng, Y., et al. (2015). Effects on murine behavior and lifespan of selectively decreasing expression of mutant huntingtin allele by supt4h knockdown. *PLoS Genet.* 11, e1005043.
- Finkel, R.S., Day, J., Chiriboga, C., Vajsar, J., Cook, D., Watson, K., Paulose, S., McMillian, L., Cruz, R., Montes, J., et al. (2014). G.O.17: results of a phase 2 open-label study of ISIS-SMNRx in patients with infantile (type 1) spinal muscular atrophy. *Neurol. Disord.* 24, 920.

32. Seth, P.P., Siwkowski, A., Allerson, C.R., Vasquez, G., Lee, S., Prakash, T.P., Wancewicz, E.V., Witchell, D., and Swayze, E.E. (2009). Short antisense oligonucleotides with novel 2'-4' conformationally restricted nucleoside analogues show improved potency without increased toxicity in animals. *J. Med. Chem.* *52*, 10–13.
33. Burel, S.A., Hart, C.E., Cauntay, P., Hsiao, J., Machermer, T., Katz, M., Watt, A., Bui, H.H., Younis, H., Sabripour, M., et al. (2016). Hepatotoxicity of high affinity gapmer antisense oligonucleotides is mediated by RNase H1 dependent promiscuous reduction of very long pre-mRNA transcripts. *Nucleic Acids Res.* *44*, 2093–2109.
34. Guo, S., Booten, S.L., Aghajan, M., Hung, G., Zhao, C., Blomenkamp, K., Gattis, D., Watt, A., Freier, S.M., Teckman, J.H., et al. (2014). Antisense oligonucleotide treatment ameliorates alpha-1 antitrypsin-related liver disease in mice. *J. Clin. Invest.* *124*, 251–261.
35. Raal, F.J., Santos, R.D., Blom, D.J., Marais, A.D., Charng, M.J., Cromwell, W.C., Lachmann, R.H., Gaudet, D., Tan, J.L., Chasan-Taber, S., et al. (2010). Mipomersen, an apolipoprotein B synthesis inhibitor, for lowering of LDL cholesterol concentrations in patients with homozygous familial hypercholesterolaemia: a randomised, double-blind, placebo-controlled trial. *Lancet* *375*, 998–1006.
36. Crooke, S.T., and Geary, R.S. (2013). Clinical pharmacological properties of mipomersen (Kynamro), a second generation antisense inhibitor of apolipoprotein B. *Br. J. Clin. Pharmacol.* *76*, 269–276.
37. Langlois, M.A., Boniface, C., Wang, G., Alluin, J., Salvaterra, P.M., Puymirat, J., Rossi, J.J., and Lee, N.S. (2005). Cytoplasmic and nuclear retained DMPK mRNAs are targets for RNA interference in myotonic dystrophy cells. *J. Biol. Chem.* *280*, 16949–16954.
38. Holt, I., Mittal, S., Furling, D., Butler-Browne, G.S., Brook, J.D., and Morris, G.E. (2007). Defective mRNA in myotonic dystrophy accumulates at the periphery of nuclear splicing speckles. *Genes Cells* *12*, 1035–1048.
39. Bassez, G., Chapoy, E., Bastuji-Garin, S., Radvanyi-Hoffman, H., Authier, F.J., Pellissier, J.F., Eymard, B., and Gherardi, R.K. (2008). Type 2 myotonic dystrophy can be predicted by the combination of type 2 muscle fiber central nucleation and scattered atrophy. *J. Neuropathol. Exp. Neurol.* *67*, 319–325.
40. Irizarry, R.A., Hobbs, B., Collin, F., Beazer-Barclay, Y.D., Antonellis, K.J., Scherf, U., and Speed, T.P. (2003). Exploration, normalization, and summaries of high density oligonucleotide array probe level data. *Biostatistics* *4*, 249–264.
41. Smyth, G.K. (2004). Linear models and empirical bayes methods for assessing differential expression in microarray experiments. *Stat. Appl. Genet. Mol. Biol.* *3*, Article3.
42. Benjamini, Y., Drai, D., Elmer, G., Kafkafi, N., and Golani, I. (2001). Controlling the false discovery rate in behavior genetics research. *Behav. Brain Res.* *125*, 279–284.
43. Wettenhall, J.M., Simpson, K.M., Satterley, K., and Smyth, G.K. (2006). affyLmGUI: a graphical user interface for linear modeling of single channel microarray data. *Bioinformatics* *22*, 897–899.
44. Vignaud, A., Ferry, A., Huguet, A., Baraibar, M., Trollet, C., Hyzewicz, J., Butler-Browne, G., Puymirat, J., Gourdon, G., and Furling, D. (2010). Progressive skeletal muscle weakness in transgenic mice expressing CTG expansions is associated with the activation of the ubiquitin-proteasome pathway. *Neuromuscul. Disord.* *20*, 319–325.
45. Dolgin, E. (2017). Spinal muscular atrophy approval boosts antisense drugs. *Nat Biotechnol.* *35*, 99–100.